

Soft Magnetic Properties and Microstructure of $\text{Ni}_{81}\text{Fe}_{19}/(\text{Fe}_{70}\text{Co}_{30})_{99}(\text{Al}_2\text{O}_3)_1$ Films Deposited by Ion Beam Sputtering

Naoto Hayashi, Yasuyoshi Miyamoto, Kenji Machida and Takahiko Tamaki

NHK Science and Technical Research Laboratories, Japan

Fax: 81-3-5494-3261, e-mail: hayashi.n-gm@nhk.or.jp

A remarkable reduction in coercivity, H_c , was found in sputtered $(\text{Fe}_{70}\text{Co}_{30})_{99}(\text{Al}_2\text{O}_3)_1$ films on Ni-Fe, Cu, Ta/Ni-Fe, or Ta/Cu underlayers. A decrease in H_c from 80 to 4-6 Oe was observed for Ni-Fe and Cu underlayers as thin as 2nm, but less for Ta. No significant difference in soft magnetic properties was observed with thickness of Ni-Fe layer in the range 0.5-10 nm or Cu layer in the range 0.2-10 nm, and with thickness of Fe-Co-Al-O layer in the range 20-500 nm. The optimized film has a saturation magnetization of 23.5 kG; the real part of the permeability shows frequencies up to 1.3 GHz of 1200-1600, and the imaginary permeability peaks at 1.7 GHz corresponding to the ferromagnetic resonance frequency. All underlayers induced a bcc-(110) preferred grain orientation in Fe-Co, which was strongest with Ta. Transmission electron microscopy of cross-sections showed that clear columnar grains were visible with all underlayers, with an average grain size of around 50 nm with Ta, dropping to 7-10 nm for Ni-Fe and Cu. This allows us to explain qualitatively the reduction in H_c using Hoffmann's ripple theory.

Key words: high-saturation magnetization, Fe-Co alloy, high frequency permeability, write head materials

1. INTRODUCTION

High saturation magnetic flux density, B_s , is a vital requirement for soft magnetic films used for recording heads, in order to achieve higher recording density. It is well documented that the highest known values occur in the bcc $\text{Fe}_{70}\text{Co}_{30}$ alloy system, with B_s of more than 24 kG. However, as-deposited Fe-Co films typically show in-plane nearly isotropic square hysteresis loops with relatively high H_c of 60-100 Oe [1]. The saturation magnetostriction is also very large with λ_s values around 5×10^{-5} . In polycrystalline films, if stresses are large, this can result in large non-uniform local magnetostrictive anisotropies and potentially high H_c . However, Wang *et al.* [2] reported that a significant reduction in H_c from 100 to 5 Oe was observed in Fe-Co-N films, and a lower H_c of 0.6 Oe was attained in films sandwiched between two Ni-Fe layers. They also proposed that increased exchange coupling between Fe-Co-N grains mediated by the Ni-Fe underlayer caused the H_c reduction. Katada *et al.* [3] reported soft magnetic properties in $\text{Fe}_{70}\text{Co}_{30}$ without the need to add nitrogen on Ni-Fe or nonmagnetic Ni-Fe-Cr, and suggested the possibility of the thin Ni-Fe layer acting as a seed layer. Shintaku *et al.* [4] also concluded that the combination of a small addition of Al_2O_3 and a soft magnetic underlayer was essential to obtain a small H_c .

In order to understand the origin of the soft magnetic properties in $(\text{Fe}_{70}\text{Co}_{30})_{99}(\text{Al}_2\text{O}_3)_1$ films, we have explored the effects of various underlayers and sputtering conditions.

2. EXPERIMENTAL PROCEDURE

Specimen Fe-Co-Al-O films with a thickness of 100 nm were deposited on Si wafer substrates with an oxidized surface using the dual ion beam sputtering (DIBS) method, a very useful and effective technique allowing independent control of the sputtering conditions. Figure 1 shows a schematic diagram of a DIBS apparatus. Both of the ion sources are Kaufman type with 5 cm diameter grids and hollow cathodes. The upper source is used for sputtering the target; the lower for bombardment of the substrate during deposition.

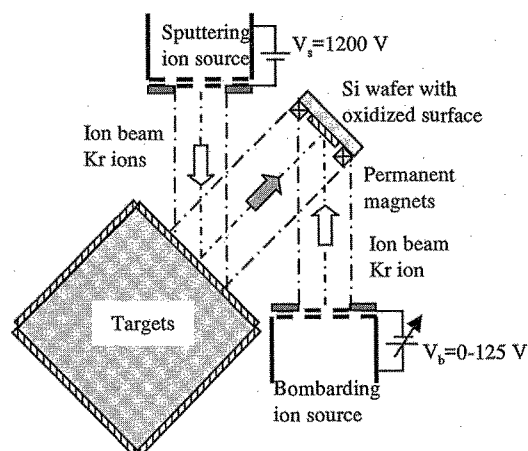


Fig.1 Schematic diagram of Dual Ion Beam Sputtering System.

Background pressure was below 4×10^{-9} Torr. Pure Kr was introduced into the sputtering and bombardment ion sources. Kr is regarded as a suitable sputtering gas for reducing the energy of recoiled particles, given that Kr ions have larger atomic mass than Ar. The compositions of the 6-inch diameter alloy targets were $(Fe_{70}Co_{30})_{99}(Al_2O_3)_1$ and $Ni_{81}Fe_{19}$. A magnetic field of 200 Oe was applied to induce an in-plane magnetic anisotropy during deposition. The films were post-annealed at 250-500 °C for an hour in an external field of 1 kOe at a pressure below 5×10^{-7} Torr.

Magnetic properties were measured using a vibrating sample magnetometer (VSM) and a cantilever-beam magnetostriction tester. High-frequency complex permeability $\mu' - j\mu''$ was measured by using a permeance meter in the frequency range of 0.01-2 GHz. The magnetic domain structure was investigated using a scanning Kerr effect microscope (SKEM) at a frequency of 0.1 MHz. Microstructure was characterized using X-ray diffractometry (XRD) with $Co-K\alpha$ radiation and transmission electron microscopy (TEM).

3. RESULTS AND DISCUSSION

Figure 2 shows typical hysteresis loops measured parallel (EA) and orthogonal (HA) to the orienting field during deposition for 100 nm thick Fe-Co-Al-O films deposited on (a) 10 nm of Ta, (b) 2 nm of Ni-Fe, (c) 2 nm of Cu, and (d) 2 nm of Ta/Ni-Fe. The films with Ta showed nearly isotropic in-plane square hysteresis loops with H_c of 80 Oe, while the films with Ni-Fe, Cu, or Ta/Ni-Fe showed well-defined uniaxial hysteresis loops with easy-axis coercivities, H_{ce} , of 8-10 Oe and hard-axis coercivities, H_{ch} , of 2-4 Oe. In these films, the anisotropy field, H_k , of around 20 Oe was found from the extrapolated hard-axis loop. The uniaxial magnetic anisotropy of the films depended strongly upon the directional order induced by an applied field during deposition, and the direction of the easy axis can be controlled by a field applied during annealing.

Figure 3 shows the Ni-Fe underlayer film thickness dependence of H_{ch} for 100 nm thick Fe-Co-Al-O films, and the insert shows hysteresis loops for the annealed film with 2nm thick Ni-Fe underlayer. The value of H_{ch} decreased dramatically upon using a Ni-Fe underlayer of thickness 0.5-10 nm, and was less than 3 Oe for the annealed films, as shown in the figure insert. The annealing temperature was set at 350 °C because the minimum of H_{ch} was found in the range 250-500 °C. No significant difference in soft magnetic properties was observed with thickness of Ni-Fe underlayer in the range 0.5-10 nm, Cu layer in range 0.2-10 nm, and Fe-Co-Al-O layer in range 20-500 nm.

As shown in Fig.4 (a)-(c), all underlayers induced a bcc-(110) preferred grain orientation in Fe-Co. The film with Ta exhibited the strongest (110) peak, indicating the possibility of larger grain size and better texture. Table I lists the values of H_{ch} , (110) lattice spacing, $d_{(110)}$, and (110) intensity, $I_{(110)}$ deposited on the underlayers of Ni-Fe, Cu, and Ta. By adding a small amount of Al_2O_3 to the Fe-Co alloy, H_c decreased with decrease in $I_{(110)}$ to one tenth of the value. Through use of a Ni-Fe or Cu underlayer, $d_{(110)}$ expanded from 2.028 to 2.036 Å, and $I_{(110)}$ decreased by a factor of five, implying reduction of grain size. Detailed characterization is required to understand the relationship between the lattice expansion and H_c reduction [5].

To better understand the relationship between the crystalline

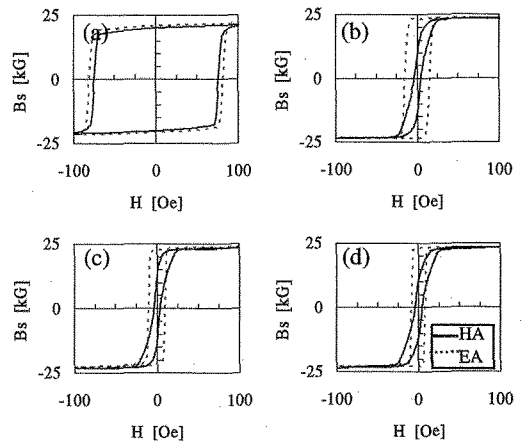


Fig.2 Typical hysteresis loops for 100 nm thick Fe-Co-Al-O films deposited on 2nm of (a) Ta, (b) Ni-Fe, (c) Cu and (d) Ta/Ni-Fe underlayers. The two different directions are parallel (EA) and orthogonal (HA) to the orienting field during deposition.

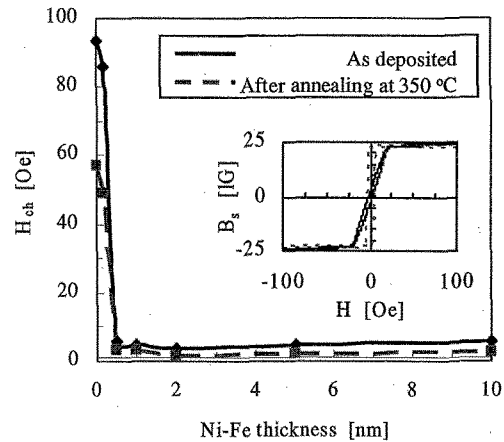


Fig.3 Ni-Fe underlayer thickness dependence of H_{ch} for 100 nm thick Fe-Co-Al-O films. The inserted figure shows hysteresis loops for the annealed film with 2 nm Ni-Fe underlayer.

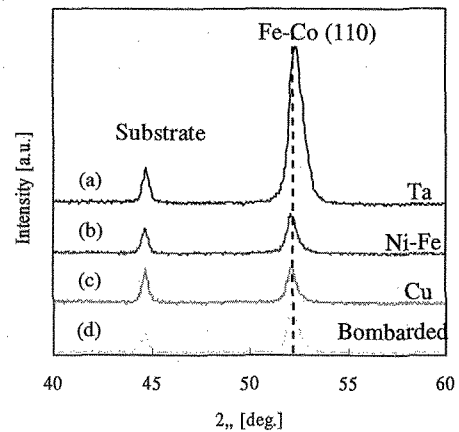
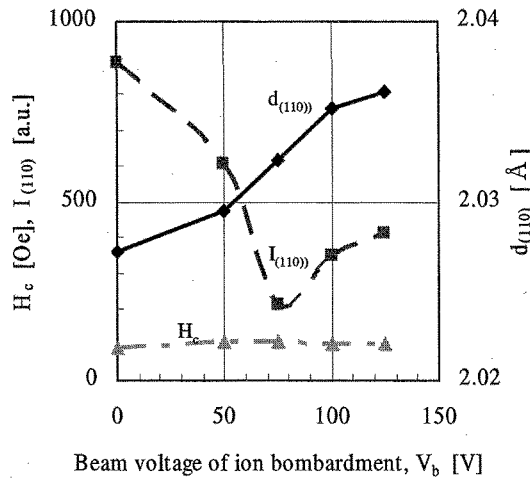


Fig.4 X-ray diffraction patterns of 100 nm thick Fe-Co-Al-O films deposited on (a) Ta, (b) Ni-Fe, (c) Cu underlayers without ion bombardment, and (d) with ion bombardment.

Table I Values of H_{ch} , $d_{(110)}$, and $I_{(110)}$ deposited on the underlayers of Ni-Fe, Cu, and Ta.

	As dep.			After annealed at 350 °C		
	H_{ch} [Oe]	$d_{(110)}$ [Å]	$I_{(110)}$ [a.u.]	H_{ch} [Oe]	$d_{(110)}$ [Å]	$I_{(110)}$ [a.u.]
Ni-Fe	3.9	2.036	287	2.0	2.033	263
Cu	4.3	2.036	233	2.0	2.033	250
Ta	75.0	2.028	1465	26.0	2.024	1453

Fig.5 Beam voltage dependence of H_c , $I_{(110)}$, and $d_{(110)}$ for Fe-Co-Al-O films deposited directly on substrate.

structure and soft magnetic properties, we investigated the effects on $d_{(110)}$, $I_{(110)}$ and H_c of ion bombardment. Figure 4 (d) shows the XRD pattern for Fe-Co-Al-O film with ion bombardment at a voltage of 100 V. Figure 5 shows the beam voltage, V_b , dependence of H_c , $d_{(110)}$ and $I_{(110)}$ for Fe-Co-Al-O film deposited directly on to substrate: it exhibits almost the same XRD pattern as for the Ni-Fe or Cu underlayer shown in Fig. 4. However, it is found that H_c exhibits no change with V_b , while the crystalline structure characterized by $d_{(110)}$ or $I_{(110)}$, perpendicular to the surface, does change with V_b . Ion bombardment may change the crystalline structure only in this direction. We believe that the in-plane crystalline structure differs for films with Ni-Fe or Cu underlayer and for bombarded films.

As shown from cross-sectional TEM images in Fig. 6, clear columnar grains were visible for all underlayers, with an average grain size of around 50 nm with Ta, dropping to 7-10 nm for Ni-Fe and Cu. In contrast, the bombarded film [Fig.6 (d)] had almost the same grain size as the film with Ta underlayer. This is one reason for the large H_{ch} value of the bombarded film.

Figure 7 shows the high-frequency complex permeability spectrum of a Fe-Co-Al-O film deposited on a 2 nm thick Ni-Fe underlayer. The film has a B_s value of 23.5 kG, H_k of 20 Oe, and μ' at frequencies up to 1.3 GHz of 1200-1600. The imaginary permeability peaks at 1.7 GHz, which corresponds to the ferromagnetic resonance frequency, f_{FMR} . The measured μ' and f_{FMR} are in relatively good agreement with the predicted value of μ' of 1070 and f_{FMR} of 1.9 GHz from the following equations [6].

$$\mu' = 1 + \frac{B_s}{H_k}, \quad (1)$$

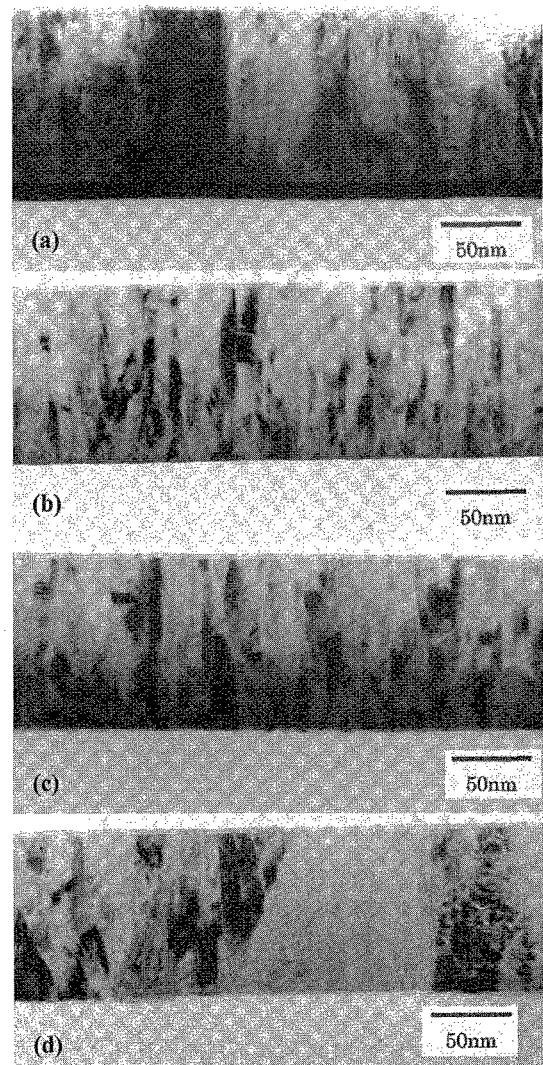


Fig.6 Cross-sectional TEM images of 100 nm thick Fe-Co-Al-O films deposited on (a) 10 nm of Ta, (b) 2nm of Ni-Fe, (c) 0.2 nm of Cu, and (d) Si substrate with ion bombardment.

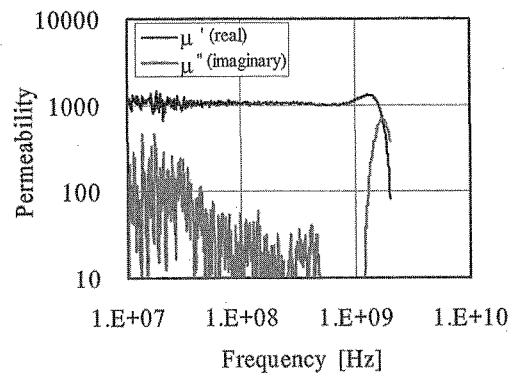


Fig.7 High-frequency complex permeability spectrum of an Fe-Co-Al-O film deposited on 2nm thick Ni-Fe underlayer.

$$f_{\text{FMR}} = \gamma \sqrt{B_s H_k}, \quad (2)$$

Where γ is the gyromagnetic ratio, all in Gaussian units. In Hoffman's ripple theory, it is practical to reduce the value of the structure factor, S , given by equation (3) in order to improve soft magnetic properties[7, 8].

$$S = K_s \sigma \frac{D}{\sqrt{N}}, \quad (3)$$

Where K_s is the local anisotropy, σ is the dispersion of the grain orientation, and N is the number of grains in the thickness. The experimental fact that λ_s of around 4×10^{-5} did not change for the films with all underlayers implies that $\lambda_{100} \approx \lambda_{111} \approx \lambda_s$. This means that $K_s \sigma$ does not depend on the film stress. Thus, it is concluded that the decrease in grain size is the main cause of the reduction in H_c for Fe-Co-Al-O films.

In order to judge practical use for recording heads, we have measured the magnetic domain structure by SKEM. Figure 8 clearly shows a periodic flux-closure pattern, normally measured in Ni-Fe or Co-Zr-Nb films with a thickness of 200 nm.

In conclusion, we have demonstrated that the primary effect of the Ni-Fe and Cu underlayer is to reduce grain size in Fe-Co-Al-O films, which causes a reduction in H_c qualitatively consistent with Hoffman's ripple theory.

References

- [1] H. Ono, M. Ishida, M. Fujinaga, H. Shishido, and H. Inaba, *J. Appl. Phys.*, 74, 5124 (1993).
- [2] S. X. Wang, N. X. Sun, M. Yamaguchi, and S. Yabukami, *Nature*, 407, 150 (2000)
- [3] H. Katada, T. Shimatsu, I. Watanabe, H. Muraoka, and Y. Nakamura, *IEEE Trans. Magn.*, 38, 2225 (2002).
- [4] K. Shintaku, K. Yamakawa, and K. Ouchi, *J. Appl. Phys.*, 93 6474, (2003).
- [5] M. Takahashi, H. Shoji, T. Shimatsu, H. Komaba, and T. Wakiyama, *IEEE Trans. Magn.*, 26, 1503 (1990).
- [6] R. M. Bozorth, "Ferromagnetism", D. Van Nostrand Co., New York, 807 (1951)
- [7] M. Takahashi, N. Kato, T. Shimatsu, H. Shouji, and T. Wakiyama, *IEEE Trans. Magn.*, 24, 3084 (1988).
- [8] H. Hoffman, *Phys. Stat. Sol.*, 33, 175 (1969)

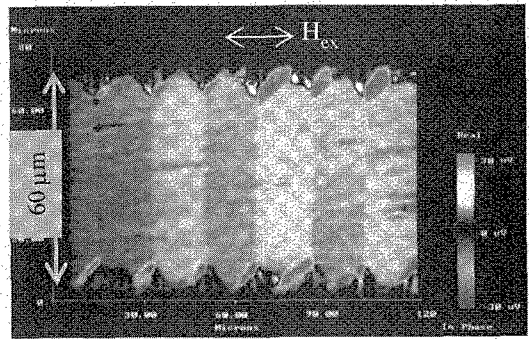


Fig.8 Observation of magnetic domains in Fe-Co-Al-O film deposited on 2nm Ni-Fe underlayer with 60 μm width. The direction of the applied field, H_{cx} , is along the hard-axis of the film.